Urban Climate 65 (2026) 102827

Contents lists available at ScienceDirect

Urban Climate

journal homepage: www.elsevier.com/locate/uclim

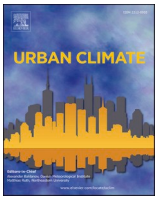

Synergistic effects of urban morphology on indoor heat and electromagnetic exposure in tropical residential remote workplaces

Flávia Brandão Ramalho de Brito [a,*], Luiz Bueno da Silva [b], Erivaldo Lopes [b], Josiane Castelo Guss [a]

[a] Department of Civil and Environmental Engineering, Federal University of Paraíba. Campus I, Castelo Branco, João Pessoa, PB 58051-900, Brazil
[b] Department of Industrial Engineering, Federal University of Paraíba. Campus I, Castelo Branco, João Pessoa, PB 58051-900, Brazil

ARTICLE INFO

Keywords:
Urban morphology
Remote workplace
Thermal comfort
Non-ionizing radiation
Sky view factor
Urban heat island

ABSTRACT

The expansion of residential remote work has intensified concerns about indoor environmental quality in dense tropical cities, where urban morphology plays a key role in shaping indoor microclimatic conditions. This study quantitatively assesses how built density, roughness, verticality, and Sky View Factor (SVF) influence operative temperature (Top) and non-ionizing radiation (NIR) exposure in 50 residential remote workplaces (RRWs) located in urban heat island areas of João Pessoa, Brazil. Morphological indicators were integrated with indoor measurements of Top (°C) and magnetic fields (μT) collected over multiple working days. Cluster analysis, multivariate statistics, and random forest models were applied to capture context-dependent effects. Random forest models showed strong performance, with R^2 values above 0.80 for both Top and NIR in low- and high-density clusters. SVF was the dominant predictor of operative temperature across all clusters, reaching relative importance values of 42.48% in low-density areas and 22.64% in dense urban fabrics. In contrast, NIR exhibited a heterogeneous response: SVF and built density dominated in open morphologies (29.22% and 23.41%), while roughness was most influential in dense contexts (26.28%). Although all NIR values remained below ICNIRP limits, 100% of RRWs exceeded the 0.4 μT benchmark commonly cited in epidemiological studies, with pronounced peaks near internal electrical transformers. The results indicate that urban morphology is statistically associated with non-linear and multiscalar variations in indoor thermal and electromagnetic exposure. These findings position urban morphology as a relevant explanatory layer for indoor environmental exposure in tropical remote-work settings, with implications for urban climate-sensitive planning and residential design.

1. Introduction

Remote work has redefined occupational environments globally, shifting attention toward the quality of residential indoor spaces as locations of prolonged daily exposure (Schulz et al., 2023). This transition emphasized the relevance of thermal comfort in dwellings that now function as improvised offices for a substantial share of the workforce (Weber et al., 2021). Unlike institutional buildings,

* Corresponding author.
E-mail addresses: flaviabrandao@pra.ufpb.br (F.B.R. de Brito), bueno@ct.ufp.br (L.B. da Silva), elopesouza@ct.ufpb.br (E. Lopes).

https://doi.org/10.1016/j.uclim.2026.102827
Received 31 October 2025; Received in revised form 3 February 2026; Accepted 6 February 2026
Available online 15 February 2026

residential spaces are highly heterogeneous and strongly shaped by their surrounding urban fabric. This aspect is particularly critical in tropical cities characterized by rapid urbanization and persistent urban heat islands (UHIs). In these settings, remote workers spend six to eight consecutive hours per day under multiple co-occurring stressors, including elevated temperatures, limited ventilation, and exposure to non-ionizing radiation, whose combined effects remain insufficiently studied (Manu et al., 2024).

Research on thermal comfort has long demonstrated the influence of environmental variables on well-being and performance (Fanger, 1970; Givoni, 1998; Larriva and Higueras, 2020), however, most evidence draws from controlled office settings (Jaiswal and Prabhakaran, 2024). Residential environments, in contrast, present greater variability due to differences in building age, construction typology, geographic location, and local urban density (Evans and Kantrowitz, 2022; Simovic et al., 2024; Jansen and Louw, 2024; Lanza and Sassi, 2022).

Parallel advances in urban climatology indicate that morphological indicators, such as roughness, verticality, and sky view factor (SVF), modulate urban microclimates by altering radiation exchange, shading, and wind flow (Emmanuel, 2005; Grimmond, 2007). These effects are non-linear and contingent on urban form heterogeneity, including variations in height and building layout (Du et al., 2020; Zoure and Genovese, 2023). For instance, Local Climate Zones LCZ-based analyses in Beijing demonstrated that SVF may correlate positively with air temperature under specific urban configurations, but its influence depends on concurrent mechanisms such as ventilation and diffuse radiation (Wang et al., 2023; Ouyang et al., 2024).

Empirical evidence suggests that reduced Sky View Factor (SVF) limits longwave radiation loss, thereby increasing nocturnal heat retention. In parallel, higher urban roughness and verticality condition airflow patterns and solar exposure. Caswell et al. (Caswell et al., 2025) reinforce that urban geometry affects residential comfort, with implications for thermal and visual conditions and human health. Despite these insights, most research has prioritized office buildings or outdoor microclimates, leaving residential workspaces underrepresented.

Simultaneously, non-ionizing radiation (NIR) has emerged as a relevant yet underexplored dimension of residential environmental quality. Magnetic fields generated by household appliances, electrical infrastructure, and digital devices represent a form of chronic, low-level exposure with potential health implications, although empirical evidence on long-term effects remains limited and often inconclusive (Nakata et al., 2021; Clegg et al., 2020; Lopez et al., 2021; Elkabany, 2023; Traini et al., 2023; Kiziloğlu et al., 2023; Meenu et al., 2025). Indoor levels depend not only on internal sources but also on external conditions that influence electromagnetic propagation (Frank, 2021). Apartments adjacent to transformer stations, for example, exhibit substantially higher magnetic-field levels than units located on higher floors (Hareuveny et al., 2011). Similarly, recent measurements in northeastern Brazil revealed peak exposures up to 17 times higher than baseline urban assessments, reaching 59–82% of ICNIRP reference levels for FM and mobile-telephony bands (Silva et al., 2025).

Prior studies have examined residential electromagnetic sources. However, the indirect influence of urban morphology on NIR exposure remains largely unexplored. Dense and vertically developed urban fabrics may increase local energy demand, while reduced Sky View Factor (SVF) and constrained ventilation can elevate indoor heat loads; together, these conditions may jointly shape thermal and electromagnetic exposure patterns (Andersen et al., 2018).

Despite extensive research on urban morphology and outdoor microclimates, alongside a growing body of literature on indoor thermal comfort and residential electromagnetic exposure, these domains have largely evolved in isolation. Existing studies rarely investigate how neighborhood-scale urban conditions simultaneously condition indoor thermal environments and non-ionizing radiation exposure, particularly within residential spaces increasingly occupied for prolonged work activities.

This gap is especially pronounced in tropical cities, where urban heat islands, high solar loads, and dense vertical development intensify indoor exposure profiles. Moreover, empirical evidence integrating operative temperature and magnetic-field measurements within real residential remote workplaces remains scarce. Addressing this gap, the present study quantitatively investigates how built density, roughness, verticality, and sky view factor jointly shaped indoor thermal conditions and non-ionizing radiation exposure in residential remote workplaces located in tropical urban heat island contexts. The research is guided by two central questions:

(i) How do morphological indicators interact to influence indoor operative temperature and NIR levels?

(ii) To what extent do these indoor conditions exceed recommended comfort and exposure benchmarks?

2. Background

2.1. Urban morphology and microclimate in tropical cities

Urban morphology encompasses the physical configuration of cities, including roughness, verticality, building density, and sky view factor (SVF), which collectively modulate urban microclimates by shaping radiation exchange, airflow, and shading patterns. In tropical cities, rapid densification and reduced open-space availability intensify spatial heterogeneity, leading to distinct microclimatic regimes that directly affect indoor thermal conditions (Emmanuel, 2005; Wei et al., 2023). Reduced SVF limits longwave radiation loss and contributes to nighttime heat retention, while increased roughness and verticality alter wind flow and solar exposure, with measurable implications for indoor environments (Wei et al., 2023).

Morphological indicators such as building coverage, built-up area, and volumetric density are positively associated with higher urban temperatures, whereas vegetation and higher SVF provide cooling effects. Fan et al. (Fan et al., 2025) reports that morphological variables can account for up to 51.2% of the spatial variability in air temperature. High-density and highly impervious areas typically exhibit elevated temperatures, while tall buildings may partially mitigate heat through shading (Zhang et al., 2024). These three-dimensional urban characteristics strongly influence occupant thermal sensation and comfort (Yang et al., 2021a) and remain central to UHI mitigation strategies in tropical regions (Deilami et al., 2018; Roth, 2013).

2.2. Indoor thermal comfort and its determinants

Thermal comfort refers to the degree of satisfaction individuals experience in their thermal environment and depends on variables such as air temperature, humidity, air movement, and mean radiant temperature. In tropical residential contexts, often without active HVAC systems, occupants are especially vulnerable to microclimate variations. Operative temperature (Top), which integrates air and radiant temperatures, is therefore a key metric for assessing indoor thermal conditions (Fanger, 1970; Givoni, 1998).

Inadequate thermal environments can compromise productivity, cognitive function, and overall health (da Silva et al., 2024). Residential comfort ranges often differ from those of office environments due to distinct expectations and behavioral adaptations (Dear and Kim, 2018). Moreover, domestic spaces exhibit wide variability in building age, location, and urban density (Evans and Kantrowitz, 2022; Jansen and Louw, 2024; Lanza and Sassi, 2022). Prolonged exposure to thermal discomfort may also influence the autonomic nervous system, increase cardiovascular risks, and impair cognitive performance (Shin and Lee, 2024).

Beyond individual factors, recent literature has highlighted the influence of urban morphology on microclimates and thermal comfort in dense urban areas. Zhang et al. (Zhang et al., 2022) demonstrated that morphological configurations significantly affect daytime thermal conditions, producing spatial heterogeneity. Similarly, Zhang et al. (Zhang et al., 2024) observed that urban verticality can enhance thermal comfort by providing effective shading. The sky view factor (SVF) has also emerged as an important determinant of thermal dissipation: higher SVF values promote cooling and reduce mean radiant temperature in urban parks (Zhang et al., 2019), while evidence from built-up areas shows correlations between SVF, shading ratio, and air temperature (Chen et al., 2023).

Despite these advances, most studies focus on outdoor environments, leaving a gap in understanding how urban morphological indicators influence indoor conditions, particularly in residences increasingly used as telework spaces.

2.3. Non-ionizing radiation in residential environments

The growing verticalization of Brazilian cities, including in the Northeast, intensifies electricity demand and expands potential sources of non-ionizing radiation (NIR). The World Health Organization (WHO) (World Health Organization, 2022) and the International Commission on Non-Ionizing Radiation Protection (ICNIRP) (International Commission on Non-Ionizing Radiation Protection, 2020) highlight the risks and exposure limits, while recent studies summarize the health effects of low-frequency fields, including sleep disorders and stress (da Silva et al., 2024; Jalilian et al., 2019; Ramirez-Vazquez et al., 2024).

The public exposure limit for NIR in the 50–300 Hz frequency range is 100 μT, according to the International Commission on Non-Ionizing Radiation Protection (ICNIRP). However, this limit is 250 times higher than 0.4 μT, a reference level frequently used in epidemiological studies that report associations between extremely low - frequency electromagnetic field (ELF -EM) exposure and potential biological effects, particularly childhood leukemia (da Silva et al., 2024; Ilonen et al., 2008; Thuróczy et al., 2008; Calvente et al., 2010; Roosli et al., 2011; Sage and Carpenter, 2012; Huss et al., 2013; Kandel et al., 2013; Zaryabova et al., 2013; Grellier et al., 2014; Struchen, 2016; Elwood, 2017). Combined analyses have indicated a consistent, albeit moderate, increase in the risk of childhood leukemia for populations exposed to these levels of non-ionizing radiation (NIR), when compared to exposures below this threshold (Ahlbom et al., 2000; Greenland et al., 2000), underscoring the need for further scientific advances in this field.

The WHO and the International Agency for Research on Cancer (IARC) have classified ELF magnetic fields as “possibly carcinogenic to humans” (Group 2B), recognizing the robustness of the epidemiological evidence, although the absence of a clearly established biological mechanism prevents definitive causal conclusions (International Agency for Research on Cancer, 2002). In terms of residential and work environments, chronic exposures above 0.4 μT, although uncommon, can occur in situations of proximity to transmission lines, transformers, or inadequate electrical installations, thus representing a relevant risk factor to be considered in the context of comfort and health in indoor environments.

NIR encompasses low-frequency electromagnetic fields emitted by electrical infrastructure, household appliances, and digital devices. In residential environments, the proliferation of Wi-Fi and Bluetooth technologies increases chronic exposure, often in spaces occupied by long telecommuting shifts. Urban morphology can modulate these levels: greater density and verticality increase electrical demand, while low SVF and limited ventilation increase indoor thermal loads, potentially altering the distribution of electromagnetic fields. However, studies integrating urban morphology, thermal comfort, and NIR exposure remain scarce (Nakata et al., 2021).

Therefore, in addition to experimental measurements, simulations are needed to understand the propagation of fields in indoor spaces, enabling more effective mitigation strategies.

2.4. Urban heat islands and their impact on residential workspaces

Global warming, combined with rapid urbanization, has intensified urban thermal stress. The replacement of natural surfaces with artificial materials such as asphalt and concrete increases daytime heat storage and reduces nighttime cooling, contributing to the formation of urban heat islands (UHIs) (Kotharkar et al., 2018). These effects are especially pronounced in tropical cities characterized by high solar radiation, limited vegetation, and low sky view factor (SVF).

UHIs exacerbate indoor heat accumulation, particularly in areas with high roughness and building density, where longwave radiation dissipation and ventilation are strongly constrained. In residential workspaces, these conditions can elevate operative temperatures and strain thermal comfort, especially in homes without active cooling systems. Although evidence directly linking UHIs to non-ionizing radiation (NIR) exposure is limited, indirect interactions may occur.

Elevated urban temperatures often increase the use of fans, air conditioners, and electronic devices, contributing to higher

electricity demand and potentially modifying residential exposure patterns. Several studies have associated these combined stressors with environmental burdens and adverse health outcomes (Han et al., 2022; He et al., 2022; Tang et al., 2025). Understanding the interplay among UHIs, urban morphology, and indoor environmental quality is therefore essential for designing thermally resilient cities and fostering healthier residential work environments (Zou et al., 2024; Yuan et al., 2025).

3. Methods

3.1. Study area

The study was conducted in João Pessoa, a coastal city in northeastern Brazil characterized by a humid tropical climate. Neighborhoods with documented heat island effects were selected (de Souza e Silva et al., 2022; Medeiros et al., 2025), encompassing areas of high building density and vertical development.

3.2. Sampling

Fifty residential remote workplaces (RRWs) were selected (Fig. 1), all located on the first three floors of residential buildings. These levels coincide with the average height of street-level transformers and are typically associated with lower natural ventilation, reduced daylighting, and greater influence from surrounding urban morphology (Haddad et al., 2024; Santamouris and Vasilakopoulou, 2023; Tregenza and Wilson, 2011). Each RRW corresponded to the primary location used for daily teleworking activities.

Restricting the sample to the first three floors introduces an expected selection bias. Both operative temperature and magnetic-field exposure may vary with elevation. However, this choice was intentional. In the typologies examined, these levels lie above the immediate thermal boundary layer at ground level while remaining sufficiently close to building surfaces, electrical components, and external infrastructures that modulate internal heat loads and magnetic-field intensities. Focusing on this potentially more exposed subset of dwellings aligns with the study's objective of examining combined thermal and electromagnetic risks within dense tropical

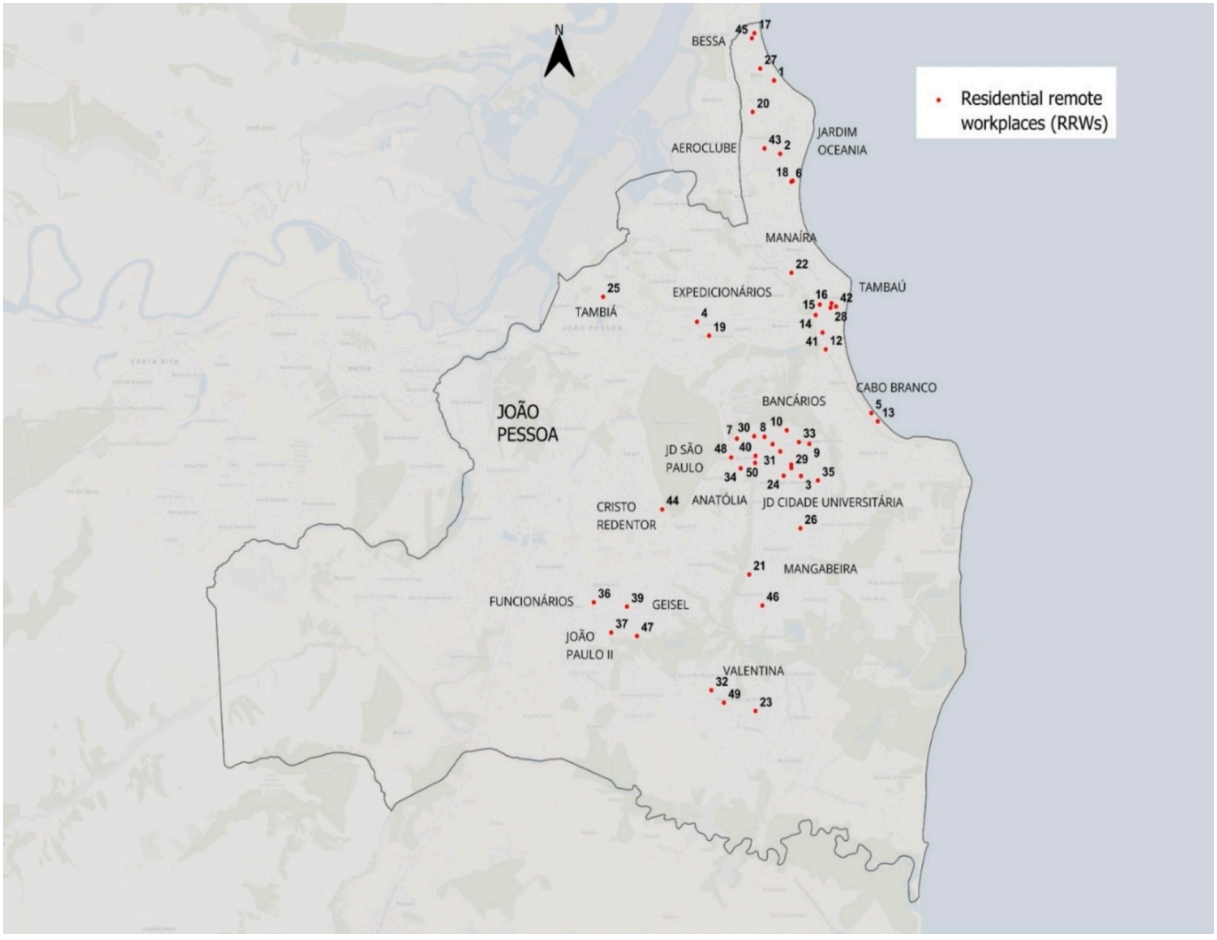

Fig. 1. Distribution of residential remote workplaces (RRWs).

morphologies.

Rather than aiming for vertical representativeness, the sampling strategy intentionally focused on lower-floor dwellings as a potentially more exposed subset, allowing the investigation of combined thermal and electromagnetic stress under conservative exposure conditions.

3.3. Data collection

Data collection followed the methodological procedures described below.

3.3.1. Internal conditions of residential remote workplaces

The operative temperature (°C) and the magnetic- field intensity - NIR (μT) were collected for three consecutive business days between 2023 and 2025, for 6 to 8 h per day, in each RRW. The operative temperature was calculated using the air temperature and the mean radiant temperature, variables measured by the TGD 400 equipment, which meets the requirements of ISO 7726 (ISO 7726, 2002) and was properly calibrated. The air velocity was considered constant, v = 0.1 m/s, an estimate for indoor environments (Coutinho, 2005; Ashrae – American Society of Heating, Refrigeration and Air Conditioning Engineers, INC, 2017). The equipment was installed in the center of the environment where remote work was performed, at approximately 0.6 m above the floor (seated occupant level).

The external climatic conditions during the data collection period were obtained from the information available on the website of the National Institute of Meteorology (*Website of National Institute of Meteorology (INMET)*, 2025), using data from the existing automatic weather stations.

The indicators of non-ionizing radiation (NIR) levels were categorized into mean, standard deviation, and maximum value. We also highlighted measurements above 0.4 μT. This value is not a regulatory or safety threshold, but a precautionary reference recurrently adopted in epidemiological studies investigating long-term exposure patterns (da Silva et al., 2024; Ilonen et al., 2008; Thuróczy et al., 2008; Calvente et al., 2010; Roosli et al., 2011; Sage and Carpenter, 2012; Huss et al., 2013; Kandel et al., 2013; Zaryabova et al., 2013; Grellier et al., 2014; Struchen, 2016; Elwood, 2017). In this study, it is used solely as a comparative benchmark to contextualize exposure levels, without implying causal or clinical risk.

The NIR data were obtained using a calibrated Aaronia USA Spectrum Analyzer, model SPECTRAN NF-5035. This equipment consists of a device capable of displaying the measured field values in real time, for the selected frequency range. The device can be connected to analysis software for real-time visualization, enabling simultaneous numerical and graphical monitoring of magnetic-field variation. The SPECTRAN NF-5035 operated within the 1–120 Hz range, and measurements focused on the 60 Hz frequency (cycles per second), which corresponds to the electrical grid frequency in Brazil, as defined by Law No. 4454/1964, Article 1 (*Website of the Federal Government's Planalto*, 2025).

Measurements were standardized at desk height (~1.1 m above floor level), with sensors positioned at least 1.0 m away from major electrical appliances and wiring whenever possible. Measurements were conducted under typical remote-working conditions, with occupants present and standard electronic equipment in operation. This approach was adopted to reflect real exposure scenarios rather than controlled laboratory conditions.

For the residential remote workplaces that exhibited mean magnetic field values substantially higher than the rest of the sample, the distance to the nearest electrical transformer was calculated. This variable was not included for all residences because these spatial data were not available for the entire sample due to limited coverage and the absence of complete public databases. However, it was used as a complementary check to assess whether proximity to external power infrastructure could explain the anomalous peak.

3.3.2. Urban morphology

Urban vector data in shapefile format, including blocks, streets, and parcels, were obtained from the João Pessoa City Hall website (*Website Prefecture of João Pessoa*, 2025). These data were processed using Geographic Information System software QGIS 2.18.2, through which maps of the study areas were generated considering a 250 m radius around each residential remote workplace.

The choice of this radius for the morphological analysis aligns with the spatial scales defined by the Local Climate Zones (LCZ) framework proposed by Stewart and Oke (Stewart and Oke, 2012). According to this classification, the characteristics of urban form and surface properties that influence local thermal behavior are best represented within approximately 200 to 500 m, a range in which urban morphology affects radiative exchange, ventilation patterns, shading, and heat storage (Mirzaei et al., 2015; Cardoso and Amorim, 2018).

These maps served as the basis for analyzing the built form, including buildings, streets, lots, vegetation, and other elements. Accordingly, the built density (dimensionless), roughness (m), verticality (m), and Sky View Factor (SVF, 0–1) indicators were derived from the urban morphological surveys and calculated using the following formulas—according to the methodology of Martins (Martins, 2020):

Built Density (D_b) - corresponds to the ratio between the sum of the useful built areas and the total area of the grid, according to Eq. (1).

$$D_b = \frac{\sum_i A_{toti}}{A} \quad (1)$$

Where A_{toti} is the totally useful constructed area of building i, and A is the total area of the studied grid.

Absolute roughness (R_a) is the average height of the urban canopy. It is given by the product of the height of buildings and their area, divided by the total area (built and unbuilt) and calculated according to Eq. (2):

$$R_a = \frac{\sum_{built} \left(A_{soil_i} \times h_{edif_1}\right)}{\sum_{built} A_{soil_i} + \sum_{unbuilt} A_{unbuilt}} \quad (2)$$

Where A_{soil_i} is the built-up area on the ground floor of the building i; h_{edif_i} is the height of the building and $A_{unbuilt}$ is the non-built area within the grid.

Verticality is defined by the built height weighted by the built area. This indicator can have a significant—and often inverse—effect on the availability of natural light on building facades (Salat, 2011).

It is calculated using the formula below (Eq. (3)):

$$V = \frac{\sum i\left(hedfi\ x\ A_{soil_i}\right)}{Asoil\ tot} \quad (3)$$

Where h_{edfi} is the height of the building i; A_{soil_i} is the built-up area on the ground floor of the building i; $A_{soiltot}$ is total built area on the ground of the grid.

To calculate the Sky View Factor (SVF), the public-domain software RayMan 3.1 (http://www.mif.unifreiburg.de/RayMan), developed by Andreas Matzarakis, was used (Matzarakis et al., 2010; Minella, 2009). The program allows the graphical representation of a given location through the insertion of fisheye images.

Hemispherical images were obtained using a low-cost fisheye lens with a 180° aperture angle, attached to an iPhone 11 Pro Max equipped with a 12-megapixel camera. During image capture, a tripod was used to standardize the height of 1.40 m, and a flat surface was used. The photos were taken on the sidewalk of the building/house under study, near the curb. For each remote work environment, at least three images were captured from different points.

The photos were processed in GIMP 2.10.36. The finalized images were inserted into RayMan software, and using the Monochrome tool, which renders obstructed areas black, it was possible to obtain estimated SVF values based on black-and-white contrast. Buildings, street furniture, and vegetation were considered obstructed areas. This methodology was supported by the authors (Matzarakis et al., 2010; Minella, 2009; Hoppe et al., 2022; De Miranda et al., 2018).

In addition to the point-based calculation of morphological indicators, spatial patterns were explored using kernel density heatmaps. Heatmaps were generated for built density, roughness, verticality, and Sky View Factor (SVF) based on the geographic coordinates of the residential remote workplaces, using each indicator as a weighting field. A consistent bandwidth of approximately 600 m and a raster resolution of 30–50 m, with data reprojected to the SIRGAS 2000/UTM Zone 25S system, were adopted to emphasize neighborhood-scale morphological gradients and hotspot formation. These maps were used as exploratory spatial tools to visualize neighborhood-scale gradients and hotspot tendencies, without implying spatial causality or point-level correspondence.

3.4. Analytical approach

The results of the internal measurements were compared with:

(i) Thermal comfort standards (Ashrae – American Society of Heating, Refrigeration and Air Conditioning Engineers, INC, 2017; *ISO* 7730:2005, 2005) and
(ii) NIR levels above 0.4 μT, a commonly used epidemiological threshold in studies investigating potential biological effects.

To investigate the relationship between indoor environmental conditions and urban morphological indicators, a multi-step statistical analysis was conducted. First, the 50 residential remote workplaces (RRWs) were grouped according to the characteristics of their surrounding urban morphology. This classification was performed using agglomerative hierarchical clustering, with Euclidean distance as the dissimilarity metric, resulting in three clusters that represent distinct morphological contexts.

After defining the clusters, it was assessed whether the four morphological metrics, built density, roughness, verticality, and Sky View Factor (SVF), differed significantly among the groups. This evaluation was carried out using Multivariate Analysis of Variance (MANOVA), applying the four conventional test statistics (Wilks' Lambda, Pillai's Trace, Hotelling–Lawley Trace, and Roy's Largest Root). In all cases, the null hypothesis of equality between at least two of the three clusters was rejected, indicating significant differences in urban morphology. Subsequently, one-way ANOVA was applied to each morphological variable, followed by Tukey's post-hoc test, which identified the specific contrasts between clusters.

Once the clusters were established, predictive modeling was performed using random forest models fitted separately for each group. The objective was to evaluate the extent to which morphological indicators could explain the indoor environmental variables: operative temperature (Top) and mean non-ionizing radiation (NIR). All models were validated using 10-fold cross-validation. Model performance was assessed through the coefficient of determination (R^2), root mean square error (RMSE), and mean bias error (MBE), allowing evaluation of both accuracy and robustness under different morphological conditions.

Finally, the relative importance of each morphological predictor was computed for all models. This analysis identified the contribution of built density, roughness, verticality, and SVF to the prediction of the environmental variables and enabled comparison of how morphological influence varied among clusters and among different metrics of thermal and electromagnetic exposure. This

multi-scale approach provided a detailed understanding of the structural influence of urban form on indoor conditions in residential remote-working environments.

4. Results

The supplementary material (table S1) summarizes all collected variables—both indoor and urban morphological—disaggregated by day and by residential remote workplace (RRW), along with the corresponding meteorological conditions for each measurement day. It also provides a detailed morphological characterization of the surroundings of each RRW (Table S2).

Before examining indoor thermal and electromagnetic conditions, the spatial distribution of urban morphological indicators was analyzed to contextualize the urban fabric surrounding the residential remote workplaces. Figs. 2–5 present kernel density heatmaps of roughness, Sky View Factor (SVF), verticality, and built density, highlighting neighborhood-scale morphological gradients and hotspot areas across the study area. Point-based maps showing the individual values of each morphological indicator at the residential remote workplaces are provided in the Supplementary Material (Figs. S1–S4) for transparency and detailed reference.

Roughness, verticality, and SVF modulate both heat accumulation and the persistence of urban electromagnetic fields, although their effects are not uniform across all environments. Higher roughness and increased building height can obstruct wind flow, reduce ventilation, and hinder heat dissipation, leading to higher surface and indoor temperatures (Wang et al., 2025). Similarly, areas with reduced SVF influence surface heat balance, air microcirculation, pollution dispersion, and overall microclimatic dynamics, thereby promoting heat accumulation (Miao et al., 2020).

These patterns are evident in the roughness and SVF heatmaps (Figs. 2 and 3), which reveal higher spatial intensities in central and coastal sectors, areas that also concentrate higher Top and NIR values at the neighborhood scale. Nevertheless, Table S1 (supplementary material) highlights marked heterogeneity among RRWs, reinforcing the need for integrated and context-sensitive analyses.

The verticality heatmap (Fig. 4) reveals clear spatial gradients, with higher concentrations of vertical development in central and coastal sectors. Areas with greater verticality, particularly in central and coastal sectors, correspond to neighborhoods previously classified as urban heat islands and tend to exhibit a higher frequency of elevated Top and NIR values. In contrast, less vertical and more dispersed areas generally show lower exposure levels, although exceptions are documented in Table S1 (Supplementary Material). These findings capture broad tendencies across the sample rather than implying a one-to-one correspondence at each measurement point.

Additionally, the built density heatmap (Fig. 5) indicates spatial concentrations of compact urban form. These locations are associated with higher Top and NIR values, suggesting that roughness, verticality, and SVF act as contextual modifiers of indoor

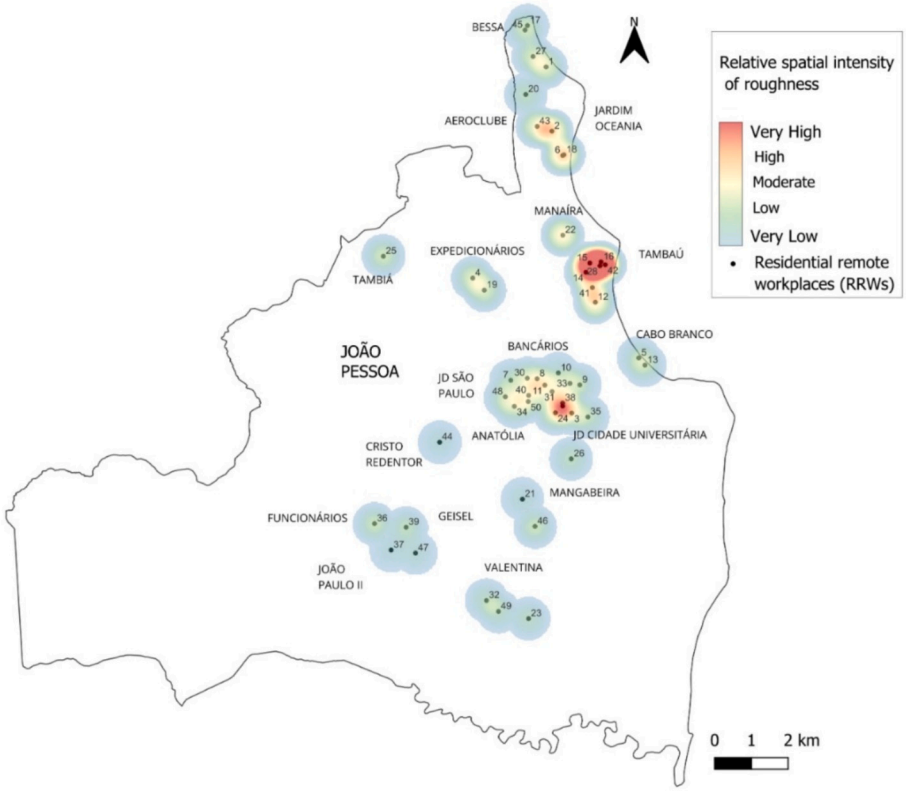

Fig. 2. Kernel density heatmap of urban roughness across the study area.

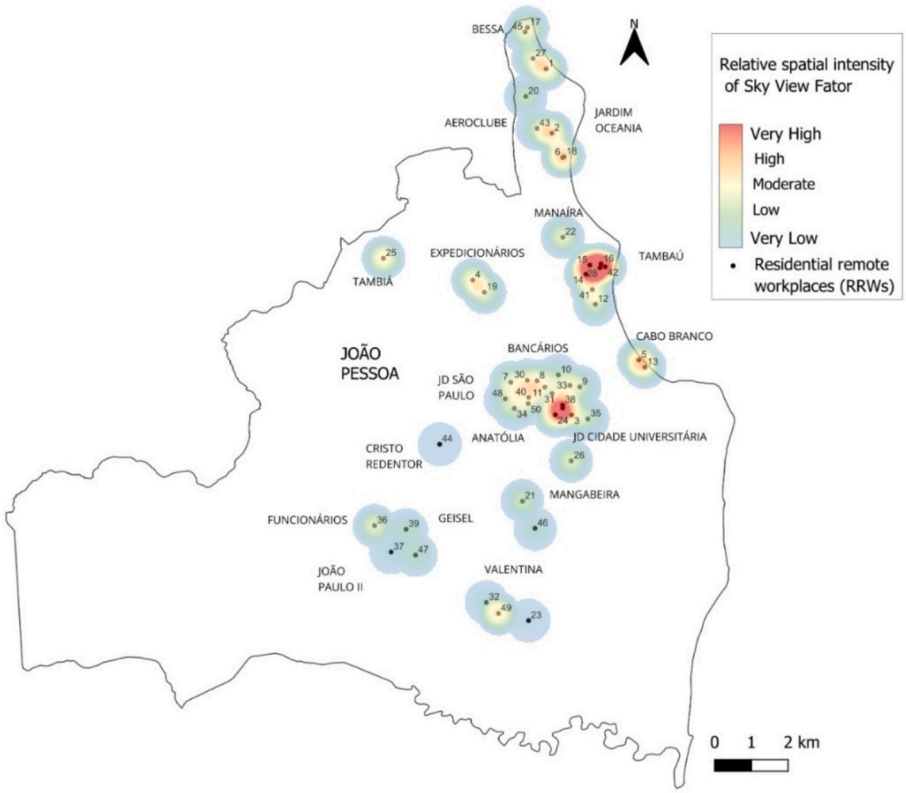

Fig. 3. Kernel density heatmap of Sky View Factor (SVF).

environmental conditions. However, Table S1 indicates heterogeneity among RRWs, with some environments exhibiting high NIR levels outside these areas, reinforcing the need to interpret these patterns as general trends rather than universal correspondences.

Spatial analysis of the maps (Figs. 2–5) reveals a consistent spatial association: areas with greater roughness and verticality, typically located in central or coastal sectors, tend to exhibit higher levels of exposure to Top and NIR. Conversely, sectors with lower roughness and higher SVF show lower exposure values. These patterns indicate that urban morphology functions as an indirect modulator of indoor environmental conditions. This factor is of growing relevance given the intensification of remote work and the consequent increase in residential exposure to urban electromagnetic fields.

It is important to highlight that exposure to non-ionizing radiation (NIR) in remote work environments located up to the third floor of buildings in neighborhoods classified as heat islands in João Pessoa, Northeast Brazil, can be influenced by both morphological attributes and broader urban characteristics. This exposure may also be affected by the evolution of mobile communication networks (3G, 4G and 5G), whose expansion entails a greater number of antennas and transmission structures. The interaction between urban form, surrounding built density, and telecommunications infrastructure underscores the importance of continuous monitoring and detailed assessment of NIR levels, particularly during periods of intense solar radiation typical of the summer season.

Thus, the results not only provide evidence for practical application in architectural projects and urban policies but also represent a significant scientific contribution by establishing a broader understanding of the relationship between urban morphology and exposure to non-ionizing radiation in residential environments, opening new avenues for future research.

4.1. Indoor conditions

4.1.1. Operative temperature in residential remote workplaces

According to Table S1 (Supplementary Material) and Graph 1, all residential remote workplaces exhibited operative temperature (Top) values above the comfort ranges recommended by international standards such as ASHRAE 55 (Ashrae – American Society of Heating, Refrigeration and Air Conditioning Engineers, INC, 2017) and ISO 7730 (*ISO* 7730:2005, 2005), which specify acceptable limits between 23 °C and 26 °C. These findings indicate that, overall, the indoor conditions of the evaluated environments do not meet international thermal comfort parameters. This result highlights the need for critical interpretation in light of specialized literature.

It is important to note that the comfort thresholds defined by ASHRAE 55 and ISO 7730 are employed herein as comparative benchmarks to contextualize observed indoor thermal conditions. Their application does not imply strict normative suitability for tropical residential environments; instead, they provide a standardized framework for the interpretative comparison of environmental performance across diverse settings.

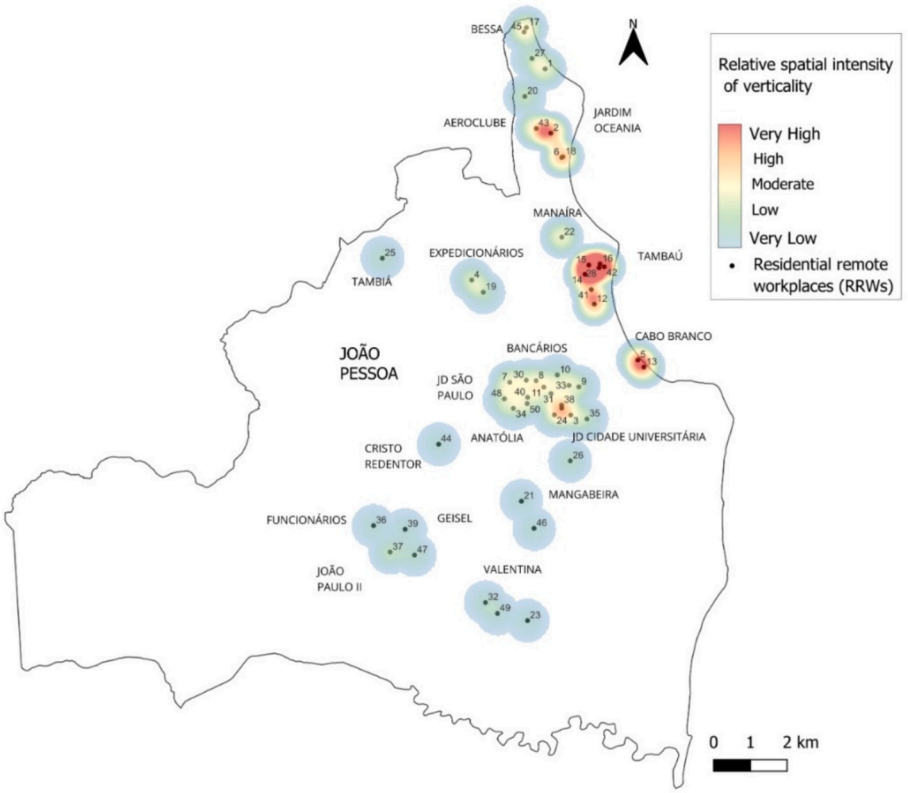

Fig. 4. Kernel density heatmap of verticality.

4.1.2. Non-ionizing radiation exposure in residential remote workplaces

All evaluated environments exhibited non-ionizing radiation (NIR) levels above the 0.4 μT reference commonly cited in epidemiological studies. Average values ranged from 1.15 μT to 8.8 μT, with 100% of the measurements exceeding this reference. Residential remote workplace (RRW) 18, located in the Bessa neighborhood, recorded the highest daily maximum values (18.79 μT; 22.18 μT; and 35.93 μT), whereas RRW 13, in the Cabo Branco neighborhood, presented the lowest (1.13 μT; 1.27 μT; and 0.60 μT). Notably, on the third day of measurement, RRW 18 reached an average of 8.8 μT and a peak of 35.93 μT (Graph 2), values substantially higher than the epidemiological reference of 0.4 μT reported in international literature as indicative of elevated exposure.

RRW 18 is located 4.33 m from an internal power transformer positioned on the second floor of the building (Fig. 6). The proximity to this electrical infrastructure likely contributes to the elevated NIR levels observed in this environment, as well as to the greater temporal variability of the measurements. Such patterns are consistent with evidence that magnetic field intensity decreases rapidly with distance from the source and may exhibit fluctuations associated with load variation in distribution equipment.

The study by Hareuveny (Hareuveny et al., 2011) shows that apartments adjacent to power transformers, especially on the first and second floors, are exposed to substantially higher magnetic- field levels than units on upper floors, classifying them as highly exposed. Indoor transformers can subject both residents and workers to elevated extremely low-frequency electromagnetic fields (ELF-EMFs), which have been associated with acute and severe health effects (Rathebe et al., 2024).

Analysis of the investigated RRWs shows that the relationship between urban morphology, thermal conditions, and non-ionizing radiation (NIR) levels is not uniform, but rather varies according to the specific characteristics of each environment.

4.2. Urban roughness and sky view factor (SVF) in the surroundings of residential remote workplaces

To facilitate comparative analyses between RRWs, a classification inspired by the studies of Salat (Salat, 2011), Oke (Oke, 1987) and Adolphe (Adolphe et al., 2002) was developed, organized based on the roughness values and the sky view factor of the present study (Table 1). This systematization aims to make the observations clearer and more comparable.

High roughness + low SVF (RRW 15): In environments located in areas of high roughness associated with low sky view factor (SVF), such as in RRW 15 (roughness of 8.52 m; verticality of 24.16 m; SVF 0.389), a significant increase in operative temperature (~30 °C) and the occurrence of NIR above 0.4 μT were observed. In addition, the high built density (2.84) compromised natural ventilation, favoring heat retention.

Moderate roughness + medium SVF (RRW 2, 6, 28): In cases of intermediate roughness and medium SVF, such as in RRW 2 (roughness 4.72 m; SVF 0.577; verticality 19.49 m), RRW 6 (roughness 2.71, SVF 0.649, verticality 9.88) and in RRW 28 (roughness

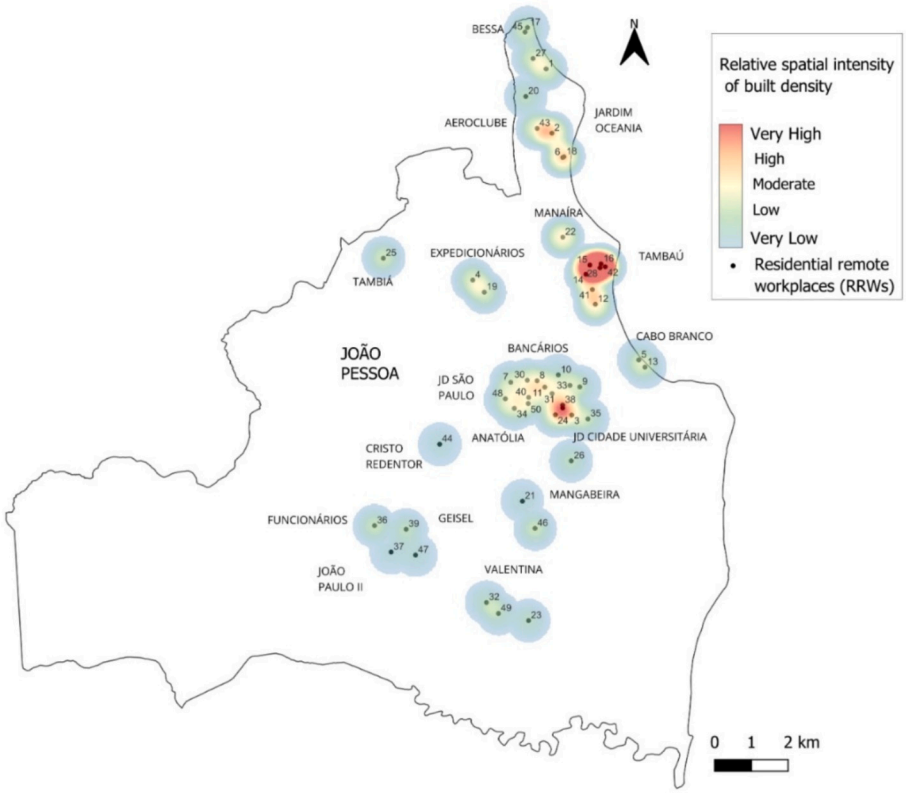

Fig. 5. Kernel density heatmap of built density across the study area.

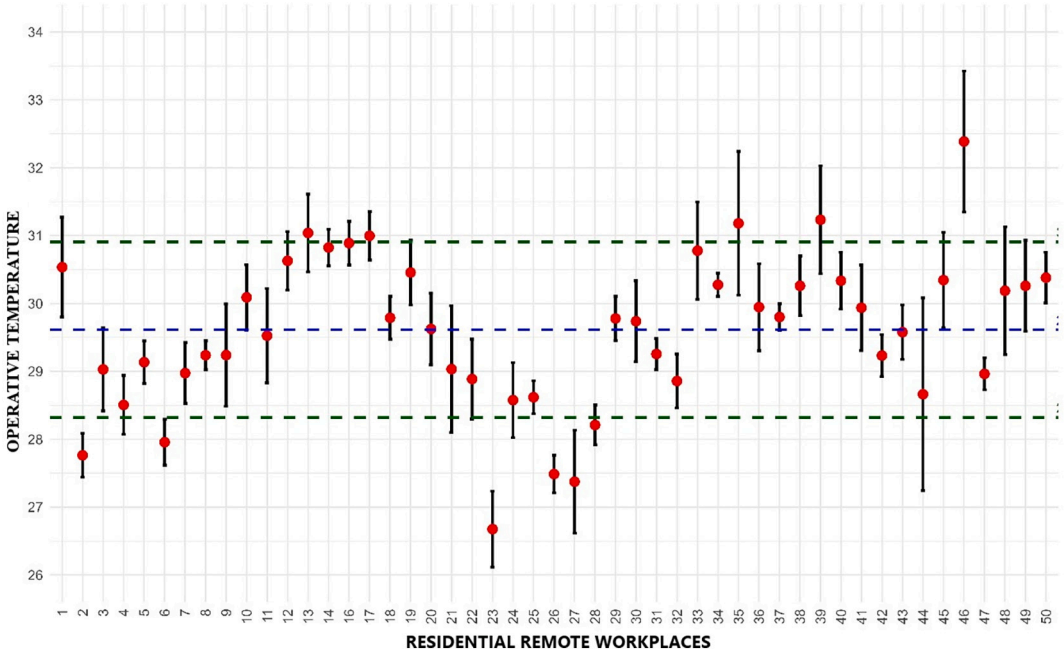

Graph 1. Average operative temperature in each RRW.

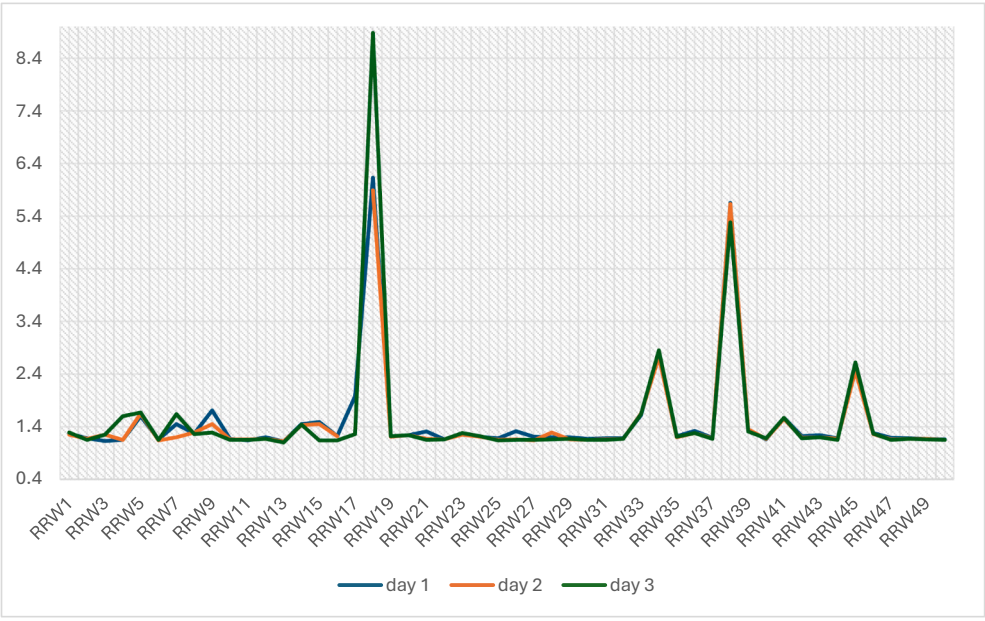

Graph 2. Average non-ionizing radiation per day for each RRWs.

Fig. 6. RRW 18 distance from the power transformer.

Table 1
Roughness and sky view factor classification.

Roughness (meters)		Sky View Factor (SVF)	
HIGH	≥ 7 m	HIGH	≥ 0.7
MODERATE	$1.8 <$ roughness<7	MODERATE	$0.4 <$ SVF < 0.7
LOW	≤ 1.8 m	LOW	≤ 0.4

5.91 m; SVF 0.645; verticality 12.91 m), the thermal conditions were a little more moderate (operative temperature ~ 28 °C), although it was still found that NIR levels were higher than 0.4 μT. The presence of heterogeneous shadows and partial ventilation suggests that, even in intermediate scenarios, there is a combination of factors that can aggravate or alleviate discomfort.

Low roughness + high SVF (RRW 37, 44, 50): Environments with low roughness and high SVF (where better indoor conditions are expected), such as RRW 37 (roughness of only 0.89 m and SVF 0.942), RRW 44 (roughness 0.98 m; SVF 0.987), and RRW 50 (roughness 1.81 m; SVF 0.959), recorded high indoor temperatures, and the entry of direct solar radiation resulted in equally high NIR levels. In these situations, low verticality (3–5 m) limited urban shading, increasing the direct incidence of solar radiation on indoor environments. Low verticality reduced shading, intensifying solar gains.

4.3. Relationship between morphological indicators and internal environmental conditions

The analysis of the descriptive measures presented in Table 2 reveals distinct patterns of urban morphology across the three identified clusters. Cluster 1 represents the least dense and most open urban context in the sample. This group shows the lowest mean values of built density, roughness, and verticality, combined with the highest mean Sky View Factor. In morphological terms, this result indicates areas with shorter, more widely spaced buildings and little height variation, characteristics that, as discussed in the literature, promote greater sky exposure, higher thermal dissipation, and reduced obstruction to natural ventilation (Yang et al., 2021b; Brandão and Barbosa, 2024). However, the results also indicate that these areas may experience greater direct incidence of solar radiation and, in some cases, greater variability in NIR associated with lower physical barriers between indoor environments and external sources (Fernández-Ahumada et al., 2019; Alfouly et al., 2025).

Cluster 2, in turn, concentrates the most critical urban conditions. The higher mean values of built density, roughness, and verticality, combined with the lowest SVF, characterize a dense, compact, and highly verticalized environment, with strong variation in building heights and limited sky openness. This pattern is consistent with the literature, which shows that denser areas tend to accumulate heat, reduce natural ventilation, and exhibit greater interference from electrical equipment and urban infrastructure (Elkhazindar et al., 2022a; Liu et al., 2022). The reduced sky view factor acts as additional modulator (Wang et al., 2023), limiting the dissipation of longwave radiation and intensifying heat retention in indoor environments.

Cluster 3 presents intermediate values for all metrics, representing a transitional morphological scenario between the two extremes. It is characterized neither by the spatial openness of Cluster 1 nor by the strong verticalization of Cluster 2, but rather by a mixed configuration, with moderate levels of density, roughness, and SVF. This condition reinforces that morphological variables do not operate in a linear manner (Wang et al., 2024), allowing intermediate environments to exhibit specific combinations of thermal and electromagnetic effects.

These results reinforce that the relationship between urban morphology, thermal comfort, and electromagnetic exposure is non-linear and multiscalar. While the internal variables (Top and NIR) tend to show a certain degree of homogeneity up to the third floor, the morphological indicators exhibit greater variability and clearly distinguish different urban scenarios (Emmanuel, 2005; Stewart and Oke, 2012). This means that even when internal conditions appear similar, the 'risk potential' of environments is deeply shaped by characteristics of the surrounding context.

Furthermore, the identification of elevated NIR levels in all investigated environments, with pronounced peaks in dwellings located near internal transformers, suggests the need for deeper discussion of the electrical infrastructure of multifamily buildings, especially

Table 2
Descriptive measures, MANOVA, and one-way ANOVA for urban metrics by clusters.

Results		Variables			
		Built density	Sky view fator	Roughness	Verticality
Descriptives measures	Cluster 1	$\bar{x}$ =0.60 (s = 0.18)	$\bar{x}$ =0.81 (s = 0.10)	$\bar{x}$ =1.80 (s = 0.54)	$\bar{x}$ =5.10 (s = 1,11)
	Cluster 2	$\bar{x}$ =1.62 (s = 0.52)	$\bar{x}$ =0.64 (s = 0.10)	$\bar{x}$ =4.87 (s = 1.57)	$\bar{x}$ =18.05 (s = 2,34)
	Cluster 3	$\bar{x}$ =1.02 (s = 0.42)	$\bar{x}$ =0.68 (s = 0.07)	$\bar{x}$ =3.01 (s = 1.31)	$\bar{x}$ =11.21 (s = 2.00)
MANOVA	Lambda de Wilks	Lambda = 0.10 (*p*-value <0.001)			
	Pillai's Trace	Trace = 0.99 (*p*-value = 0.001)			
	Hotteling - Lawleys's Trace	Trace = 8.52 (*p*-value <0.001)			
	Roy's Root	Root = 8.41 (p-value <0.001)			
One Factor ANOVA		F = 1440.25 (p-value <0.001)	F = 603.96 (p-value <0.001)	F = 1384.26 (p-value <0.001)	F = 9837.35 (p-value <0.001)

considering the expansion of remote work and the prolonged occupancy of these spaces. The literature has warned that chronic exposures above 0.4 μT (a recurrent reference in epidemiological studies) may be associated with potential biological effects, particularly risks related to childhood leukemia (Ilonen et al., 2008; Thuróczy et al., 2008; Calvente et al., 2010; Roosli et al., 2011; Sage and Carpenter, 2012; Huss et al., 2013; Kandel et al., 2013; Zaryabova et al., 2013; Grellier et al., 2014; Struchen, 2016; Elwood, 2017). Although this is not a causal threshold, the finding that 100% of the sample presented values above this reference highlights the relevance of preventive policies and continuous monitoring.

After defining the clusters based on urban morphology indicators, random forest models were fitted separately for each group. Table 3 presents the performance metrics of the random forest models fitted for each cluster, using 10-fold cross-validation. The results indicate that the models achieved good overall performance, especially in Clusters 1 and 2, which exhibited R^2 values above 0.80 for both operative temperature (Top) and mean non-ionizing radiation (NIR). The model for Cluster 3 showed a slightly lower R^2 for Top (0.7130), but still within a range considered acceptable for environmental analyses in heterogeneous urban scenarios.

The consistent model performance across clusters indicates that the selected morphological indicators capture structurally meaningful patterns rather than spurious correlations, supporting their interpretability in urban climate assessments. The RMSE values further reinforce the quality of the model fit. For operative temperature, RMSE ranged from 0.4166 °C to 0.7388 °C, which are relatively low when compared to the range of the observed records, exceeding 29 °C.

For NIR, RMSE varied between 0.0468 μT (Cluster 2) and 0.4468 μT (Cluster 1), remaining similarly low in relation to the empirical variability of the variable. The MBE was close to zero across all models, indicating no systematic bias in the estimates. These results demonstrate that the random forest models were able to adequately capture the relationship between indoor environmental variables (Top and NIR) and urban morphology indicators in each surrounding context.

Based on the performance results presented in Table 3, the analysis then proceeded to the assessment of the relative importance of morphological metrics for each group, allowing the identification of how built density, roughness, verticality, and SVF influence operative temperature and non-ionizing radiation levels in residential remote-work environments.

The results show, as presented in Table 4, that no single indicator acts in isolation, with a distinct composition of influences observed according to the urban context represented by the clusters. For operative temperature (Table 4 and Fig. 7), it is observed that the Sky View Factor (SVF) exhibited high relative importance in all clusters, especially in Cluster 1 (42.48%) and Cluster 2 (22.64%). This finding is consistent with the role of SVF in modulating heat dissipation (Middel et al., 2018).

In the case of non-ionizing radiation, the distribution of importance was again distinct across clusters (Table 4 and Fig. 8), indicating variations in how the urban surroundings modulate indoor electromagnetic fields. In Cluster 1, SVF and built density were the most influential indicators (29.22% and 23.41%, respectively), suggesting that areas with greater sky openness and lower density may favor higher variability in the propagation of external electromagnetic fields.

For Cluster 2, roughness emerged as the most influential indicator (26.28%), reflecting the influence of more complex built forms, typical of dense and highly verticalized areas, which may affect the reflection, absorption, and attenuation of electromagnetic fields. In Cluster 3, the importance of the indicators showed a more homogeneous distribution, with values close to one another, indicating a morphologically less contrasted environment in which NIR is modulated by multiple factors simultaneously.

In this way, the results reinforce that the effects of urban morphology on indoor environmental conditions are contextual, varying according to the spatial pattern of the surrounding environment in which each RRW is embedded. The interaction among SVF, density, roughness, and verticality is fundamental; however, the relative weight of each metric changes across clusters, suggesting that different urban configurations generate distinct mechanisms of thermal accumulation and modulation of electromagnetic fields.

4.4. General standards

The observed homogeneity in internal thermal conditions and non-ionizing radiation (NIR) up to the 3rd floor should not be viewed as a limitation but as a relevant methodological finding. Previous studies indicate that, beyond a certain height, microclimatic variables tend to stabilize due to reduced influence from ground-level and adjacent surfaces (Emmanuel, 2005; Stewart and Oke, 2012; Oke, 1987; Roth, 2007), and that electromagnetic fields decrease with distance from their sources (*ICNIRP*, 2020; Kljajic et al., 2025). The results empirically reinforce this evidence and validate the decision to limit measurements to the first three floors.

The contrast between the local homogeneity of thermal and NIR values and the heterogeneity of morphological indicators highlights differences in spatial and temporal scales: while environmental measurements capture short-term stabilized conditions, morphological indicators reflect long-lasting structural characteristics of the urban fabric. This distinction deepens the understanding of how built form influences comfort in remote residential workplaces and suggests that morphological variables, due to their greater variability, may serve as predictors for scenarios beyond the current measurement framework (e.g., other floors or urban typologies).

Comparisons across the 50 RRWs also indicate that morphological indicators do not operate independently but act through combined and overlapping mechanisms. Areas with high roughness and low SVF showed amplified heat stress and elevated NIR levels, whereas high-SVF locations, despite improving ventilation and reducing heat accumulation, exhibited greater direct solar exposure due to reduced shading.

5. Discussion

5.1. Comparison with international evidence

Building on the cluster-based results and the relative importance analysis presented in Section 4, the discussion highlights the

Table 3
Model performance metrics obtained using 10-fold cross-validation.

Variables	Metric	Cluster 1	Cluster 2	Cluster 3
Operative temperature	R^2	0.8130	0.8792	0.7130
	RMSE	0.5109	0.4166	0.7388
	MBE	0.0002	−0.0038	−0.0008
Non-ionizing radiation	R^2	0.9113	0.9022	0.9329
	RMSE	0.4468	0.0468	0.1165
	MBE	−0.0003	−0.0004	−0.0002

Table 4
Degree of importance of urban morphology metrics.

Response Variable	Predictors	Importance level		
		Cluster 1	Cluster 2	Cluster 3
Operative temperature	Built density	38.02	20.13	26.78
	Sky view factor	42.48	22.64	24.18
	Roughness	34.17	19.90	21.49
	Verticality	39.48	18.72	26.65
Non-ionizing radiation	Built density	23.41	24.33	25.19
	Sky view factor	29.22	23.28	28.96
	Roughness	23.01	26.28	25.23
	Verticality	22.43	19.83	24.62

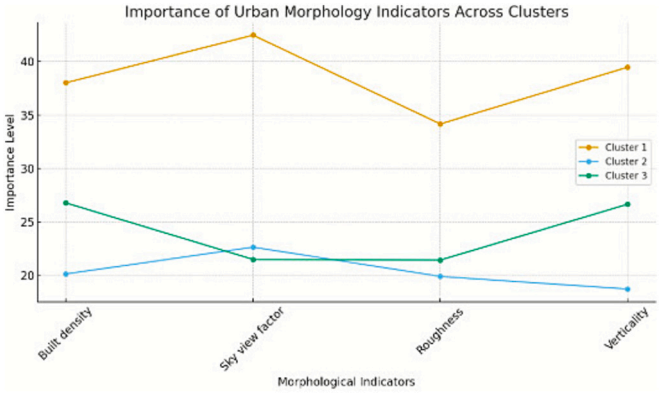

Fig. 7. Degree of importance of urban morphology metrics for Top.

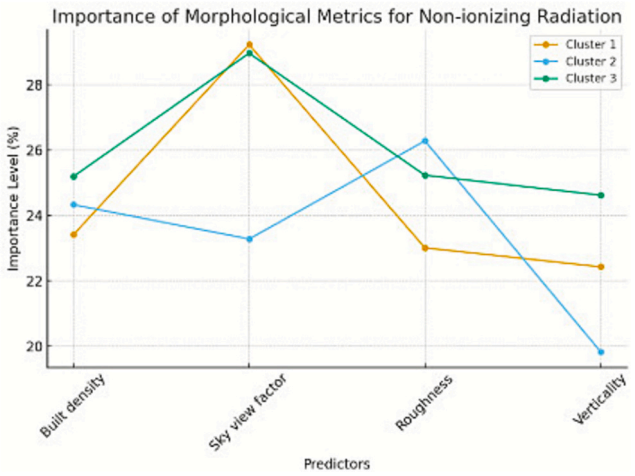

Fig. 8. Degree of importance of urban morphology metrics for NIR.

complex interaction between urban morphology and indoor environmental conditions in residential remote workplaces (RRWs).

RRWs located in areas of high roughness and low SVF, representative of Cluster 2, consistently exhibited operative temperatures above 29 °C and NIR levels above 0.4 μT. This combination of high urban density and limited ventilation simultaneously intensifies thermal and electromagnetic stress. These findings corroborate previous studies that associate reduced SVF and increased urban density with higher thermal stress (Emmanuel, 2005; Grimmond, 2007). These values are consistent with findings from tropical high-density cities such as the United Arab Emirates (Elkhazindar et al., 2022b), where reduced SVF and compact urban canyons intensify indoor overheating and constrain daytime ventilation. The magnitude of indoor overheating observed in dense clusters (>29 °C) is comparable to values reported for compact tropical cities such as Singapore, Bangkok, and Gulf-region urban districts, reinforcing the external relevance of the findings.

Data analysis also reveals that the location of the environment within the urban fabric directly and indirectly influences thermal comfort and NIR levels. Near urban electrical sources, such as transformers, distribution networks, or high-power equipment, RRWs recorded NIR values significantly higher than 0.4 μT, as observed in RRW 18, which showed peaks of up to 35.93 μT, indicating that urban morphology is not neutral and that urban electrical infrastructure can generate risks associated with prolonged exposure (Hareuveny et al., 2011).

In intermediate scenarios (RRWs 2, 6, and 28), thermal conditions were more moderate (~28 °C), but NIR levels remained high throughout the collection period. The combination of partial ventilation and heterogeneous shading highlights the combined effect of roughness, verticality, and SVF on the indoor environment.

On the other hand, RRWs located in areas of low roughness and high SVF (RRWs 44 and 50) showed greater thermal dissipation due to more efficient ventilation, but direct solar exposure increased thermal and NIR levels above 0.4 μT. This observation is consistent with the relative importance analysis, which showed that although SVF plays a key role in modulating operative temperature, its effects are mediated by density, roughness, and verticality, particularly in Cluster 3. These results are in line with (Nakata et al., 2021; Havenith, 2019; Yu et al., 2020; Shankar and Sundaram, 2025), emphasize integrated approaches to optimize thermal comfort while reducing electromagnetic exposure (Chiaramello et al., 2019).

The comparison across morphological contexts confirms that urban form conditions indoor thermal and electromagnetic exposure through multiple interacting pathways. In low-SVF areas, ventilation deficits restrict heat dissipation and increase reliance on internal loads, amplifying operative temperatures. Simultaneously, electrical infrastructure embedded within dense urban fabrics—particularly transformers and distribution networks—can elevate NIR levels, as observed in RRW 18 (peak 35.93 μT).

In high-SVF areas, increased sky exposure enhances radiative exchange but also increases direct solar incidence and potential EMF transmission from nearby telecommunications and power equipment. The contrast between RRW 15 (SVF = 0.389) and RRW 44 (SVF = 0.987) reinforces that neither extreme ensures comfort; rather, thermal and electromagnetic responses reflect nonlinear interactions between roughness, verticality, and SVF.

5.2. Implications for exposure limits and urban health

Consistent with the results presented in Section 4, which showed that all investigated RRWs exceeded the 0.4 μT reference level, the discussion highlights that exposure concerns emerge even when ICNIRP limits are not surpassed. Several RRWs exceeded levels above 0.4 μT, considered exposure levels that warrant precautionary consideration in the context of prolonged residential occupancy as well as exceeded comparative precautionary benchmarks proposed by EUROPAEM (2016) and the Building Biology Standard (SBM-2015), which recommend thresholds an order of magnitude lower for chronic exposure in residential settings. This indicates that even when regulatory limits are not exceeded, remote workers in compact tropical morphologies may experience exposure profiles that warrant further scientific investigation. The findings underscore the need for integrating EMF considerations into microclimate-driven building and planning strategies, especially in rapidly densifying tropical cities.

5.3. Synergistic thermal–electromagnetic stress and occupational health implications for remote workers

Remote work amplifies the importance of indoor environmental quality by extending daily exposure windows to 6–8 h in a single location. In dense tropical morphologies, thermal stress and electromagnetic exposure do not operate independently. Limited ventilation, high humidity, and intense radiant loads can reduce the capacity for physiological heat dissipation, while co-occurring exposure to elevated magnetic fields may interact with thermal fatigue, discomfort, and cognitive strain. Although synergistic effects are not fully understood, the overlap of these stressors suggests potential compound risks for remote workers. These risks are particularly relevant in dwellings located near electrical infrastructure or within dense, low-SVF urban blocks.

It is important to note that, in this study, the term “synergistic effects” refers to the concurrent and reinforcing presence of multiple urban morphological factors that collectively influence indoor thermal environments and non-ionizing radiation exposure. This conceptual framework emphasizes the convergence of environmental pressures within residential remote work settings, rather than the formal modeling of statistical interaction terms.

Taken together, the three morphological clusters represent distinct but interconnected exposure regimes, in which thermal and electromagnetic stressors overlap in different intensities, reinforcing the need for integrated urban and building-scale mitigation strategies. These findings reinforce the need for ergonomic and urban policy frameworks that incorporate both thermal and electromagnetic dimensions, guiding building retrofits, zoning decisions, and workplace recommendations for the rapidly expanding population of remote workers in tropical cities.

6. Conclusions

This study investigated how urban morphology modulates indoor thermal conditions and non-ionizing radiation (NIR) exposure in residential remote workplaces (RRWs) within a tropical context. By integrating cluster analysis, multivariate statistics, and machine learning models, the results provide robust quantitative evidence that indoor environmental conditions are strongly shaped by the surrounding urban fabric rather than by indoor characteristics alone. The main conclusions are as follows:

- Urban morphology exerts a statistically significant and measurable influence on both operative temperature (Top) and NIR. Random forest models achieved R^2 values above 0.80 for most clusters, demonstrating that built density, roughness, verticality, and Sky View Factor (SVF) explain a substantial share of indoor environmental variability, even when internal conditions appear similar.
- SVF emerged as the most influential predictor of operative temperature across all clusters, reaching 42.48% of relative importance in low-density contexts and 22.64% in dense urban fabrics. However, high SVF did not uniformly improve thermal comfort, as increased sky exposure also intensified direct solar gains. This confirms that SVF operates as a key but non-sufficient parameter, whose effects depend on its interaction with density, roughness, and verticality.
- Clusters characterized by high built density, roughness, and verticality combined with low SVF consistently exhibited the most critical indoor conditions, with operative temperatures frequently exceeding 29 °C and elevated NIR levels. These environments also showed the strongest influence of roughness on NIR (up to 26.28% relative importance), indicating that compact urban forms amplify thermal accumulation and electromagnetic exposure through overlapping mechanisms.
- Intermediate morphological contexts showed no dominance of a single indicator, with Top and NIR shaped by the simultaneous interaction of multiple metrics. This balanced distribution of variable importance confirms the non-linear and multiscalar nature of morphology–indoor environment relationships and supports the use of machine learning approaches to capture such complexity.
- Although all measured NIR values remained below ICNIRP reference limits, 100% of the RRWs exceeded the 0.4 μT benchmark commonly cited in epidemiological literature. The 0.4 μT value referenced in this study is intended as an epidemiological benchmark for contextualizing exposure levels, rather than a regulatory or deterministic threshold for health risks. Its inclusion serves to facilitate the analysis of observed data while acknowledging the ongoing scientific debate and the inherent uncertainties regarding the long-term biological implications of non-ionizing radiation exposure. Pronounced NIR peaks, reaching up to 35.93 μT, were observed in dwellings near internal electrical transformers, highlighting the role of building-scale electrical infrastructure in shaping exposure profiles, particularly under extended remote work durations.
- The findings demonstrate that improving indoor environmental quality in tropical cities requires morphology-aware strategies beyond the building scale. From an urban climate perspective, the results support morphology-aware planning strategies that integrate ventilation potential, controlled sky exposure, and careful placement of electrical infrastructure to mitigate combined indoor heat and electromagnetic exposure in tropical cities.

CRediT authorship contribution statement

Flávia Brandão Ramalho de Brito: Writing – review & editing, Writing – original draft, Supervision, Project administration, Methodology, Investigation, Formal analysis, Conceptualization. **Luiz Bueno da Silva:** Visualization, Validation, Supervision, Resources, Methodology, Investigation, Data curation, Conceptualization. **Erivaldo Lopes:** Writing – review & editing, Validation, Software, Conceptualization. **Josiane Castelo Guss:** Software, Methodology.

Declaration of competing interest

The authors declare that they have no known competing financial interests or personal relationships that could have appeared to influence the work reported in this paper.

Acknowledgments

The authors would like to express sincere thanks to everyone who contributed to this work, including the National Council for Scientific and Technological Development, which funded this research.

Appendix A. Supplementary data

Supplementary data to this article can be found online at https://doi.org/10.1016/j.uclim.2026.102827.

Data availability

Data will be made available on request.

References

Adolphe, L., et al., 2002. SAGA Cités Vers un Système d'Aide à la Gestion des Ambiances urbaines. MENRT, Toulouse.

Ahlbom, A., Day, N., Feychting, M., Roman, E., Skinner, J., Dockerty, J., Linet, M., 2000. A pooled analysis of magnetic fields and childhood leukaemia. Br. J. Cancer 83 (5), 692–698. https://doi.org/10.1054/bjoc.2000.1262.

Alfouly, M., Halilovic, S., Hamacher, T., 2025. Evaluating urban form influence on solar exposure and corresponding building energy demands. Energ. Buildings 338, 115708. https://doi.org/10.1016/j.enbuild.2025.115708.

Andersen, J.B., Rappaport, T.S., Yoshida, S., 2018. Propagation Measurements and Models for Wireless Communications Channels. IEEE Press.

Ashrae – American Society of Heating, Rrefrigeration and Aair Cconditioning Eengineers, INC, 2017. Standard 55: Thermal Environmental Conditions for Human Occupancy. Atlanta.

Brandão, L.K. de V., Barbosa, R.V.R., 2024. Efeitos da rugosidade superficial na variabilidade da ventilação natural em cânions urbanos, em clima tropical de savana. Rev. Nac. Gerenc. Cid. 12 (86). https://doi.org/10.17271/23188472128620245307.

Calvente, I., Fernandez, M.F., Villalba, J., Olea, N., Nuñez, M.I., 2010. Exposure to electromagnetic fields (non –ionizing radiation) and its relationship with childhood leucemia: A systematic review. Sci. Total Environ. 408 (16), 3062–3069. https://doi.org/10.1016/j.scitotenv.2010.03.039.

Cardoso, R.S., Amorim, M.C.C.T., 2018. Urban heat island analysis using the 'local climate zone' scheme in Presidente Prudente, Brazil. Investig. Geogr. 69, 107–118. https://doi.org/10.14198/INGEO2018.69.07.

Caswell, H., Alidoust, S., Corcoran, J., 2025. Planning for livable compact vertical cities: a quantitative systematic review of the impact of urban geometry on thermal and visual comfort in high-rise precincts. Sustain. Cities Soc. 119. https://doi.org/10.1016/j.scs.2024.106007.

Chen, Q., et al., 2023. Evaluating the impact of sky view factor and building shadow ratio on urban air temperature. Build. Environ. 233, 110043. https://doi.org/10.1016/j.buildenv.2023.110043.

Chiaramello, E., Bonato, M., Fiocchi, S., Tognola, G., Parazzini, M., Ravazzani, P., Wiart, J., 2019. Radio frequency electromagnetic fields exposure assessment in indoor environments: a review. Int. J. Environ. Res. Public Health 16 (6), 955. https://doi.org/10.3390/ijerph16060955.

Clegg, F.M., Sears, M., Friesen, M., Scarato, T., Metzinger, R., Russell, C., Stadner, A., Miller, A.B., 2020. Building science and radiofrequency radiation: what makes smart and healthy buildings, 176 (2020), 106324. https://doi.org/10.1016/j.buildenv.2019.106324.

Coutinho, A.S., 2005. Conforto e insalubridade térmica em ambientes de trabalho. Editora Universitária, João Pessoa. ISBN:85.237.126–5.

da Silva, Luiz Bueno, Melo, Carmem Julianne Beserra, Souza, Adriana.G. Lisboa, de Oliveira, Lucas Guedes, 2024. Ergonomics, health, and perceptions about remote domestic workposts: study in areas of City of João Pessoa, Paraíba, Brazil. Int. J. Environ. Res. Public Health 21, 1–23 (ISSN 1660-4601).

De Miranda, S.A., et al., 2018. Analysis of an alternative proposal for obtaining the sky view factor using a photographic method. Braz. J. Climatol. 23.

de Souza e Silva, R., da Silva, R.M., de Freitas, A.F., et al., 2022. Thermal comfort conditions at microclimate scale and surface urban heat island in a tropical city: a study on João Pessoa city, Brazil. Int. J. Biometeorol. 66, 1079–1093. https://doi.org/10.1007/s00484-022-02260-y.

Dear, R.D., Kim, J., 2018. Thermal comfort expectations and adaptive behavioural characteristics of primary and secondary school students. Build. Environ. 126, 1–10. https://doi.org/10.1016/j.buildenv.2017.10.031.

Deilami, K., Givoni, B., Shashua-Bar, L., 2018. Urban heat island effect: A systematic review of spatio-temporal factors, data, methods, and mitigation measures. Renew. Sust. Energ. Rev. 81, 2002–2018. https://doi.org/10.1016/j.rser.2017.08.033.

Du, S., Li, Y., Wang, C., Tian, Z., Lu, Y., Zhu, S., Shi, X., 2020. A cross-scale analysis of the correlation between daytime air temperature and heterogeneous urban spaces. Sustainability 12, 7663. https://doi.org/10.3390/su1218766.

Elkabany, S.N., 2023. Study the effect of electromagnetic radiation towards sustainable healthy buildings. J. Eng. Sci. Inf. Technol. 7 (1), 69–79. https://doi.org/10.26389/AJSRP.Q191222.

Elkhazindar, A., Kharrufa, S.N., Arar, M.S., 2022a. The effect of urban form on the heat island phenomenon and human thermal comfort: a comparative study of UAE residential sites. Energies 15 (15), 5471. https://doi.org/10.3390/en15155471.

Elkhazindar, A., Kharrufa, S.N., Arar, M.S., 2022b. O efeito da forma urbana no fenômeno da ilha de calor e no conforto térmico humano: um estudo comparativo de áreas residenciais nos Emirados Árabes Unidos. Energies, 5471. https://doi.org/10.3390/en15155471.

Elwood, M., 2017. Epidemiological studies of low –intensity ELF fields and diseases in humans. In: Wood, Andrew W., Karipidis, Ken (Eds.), Non-ionizing – Radiation Protection, 20. Wiley, USA, pp. 313–321. https://doi.org/10.1002/9781119284673.ch20.

Emmanuel, R., 2005. An Urban Approach to Climate Sensitive Design: Strategies for the Tropics. Taylor & Francis, London.

Evans, G.W., Kantrowitz, E., 2022. Residential building age and its impact on thermal comfort and indoor environmental quality. Environ. Res. Lett. 17 (5), 054021. https://doi.org/10.1088/1748-9326/ac5a0e.

Fan, J., Chen, X., Xie, S., Du, K., 2025. Mediating effect of air pollutants on urban morphology and air temperature. Atmos. Pollut. Res. 16 (4), 102426. https://doi.org/10.1016/j.apr.2025.102426.

Fanger, P.O., 1970. Thermal Comfort: Analysis and Applications in Environmental Engineering. McGraw-Hill, New York.

Fernández-Ahumada, L.M., Ramírez-Faz, J., López-Luque, R., Márquez-García, A., Varo-Martínez, M., 2019. A methodology for buildings access to solar radiation in sustainable cities. Sustainability 11 (23), 6596. https://doi.org/10.3390/su11236596.

Frank, J.W., 2021. Electromagnetic fields, 5G and health: what about the precautionary principle? Epidemiol. Community Health 75, 562–566. https://doi.org/10.1136/jech-2019-213595.

Givoni, B., 1998. Climate Considerations in Building and Urban Design. Wiley, New York.

Greenland, S., Sheppard, A.R., Kaune, W.T., Poole, C., Kelsh, M., 2000. A pooled analysis of magnetic fields, wire codes, and childhood leukemia. Epidemiology 11 (6), 624–634. https://doi.org/10.1097/00001648-200011000-00003.

Grellier, J., Ravazzani, P., Cardis, E., 2014. Potential health impacts of residential exposures to extremely low frequency magnetic fields in Europe. Environ. Int. 62, 55–63. https://doi.org/10.1016/j.envint.2013.09.017.

Grimmond, C.S.B., 2007. Urbanization and Climate: Modeling the Surface Energy Balance of Urban Areas. Cambridge University Press, Cambridge.

Haddad, S., et al., 2024. Quantifying the energy impact of heat mitigation technologies at the urban scale. Nat. Cities 1, 62–72.

Han, J., Zhang, X., Li, Y., 2022. Impact of urban heat islands on morbidity and mortality in urban areas: a systematic review. Sci. Total Environ. 827, 154382. https://doi.org/10.1016/j.scitotenv.2022.154382.

Hareuveny, R., Kandel, S., Yitzhak, N.M., et al., 2011. Exposure to 50 Hz magnetic fields in apartment buildings with indoor transformer stations in Israel. J. Expo. Sci. Environ. Epidemiol. 21, 365–371. https://doi.org/10.1038/jes.2010.20.

Havenith, G., 2019. Thermal comfort and climate change. Build. Res. Inf. 47 (4), 351–356.

He, Y., Li, Z., Liu, J., 2022. A systematic review of urban heat island and heat waves interactions: implications for public health. Sci. Total Environ. 832, 154981. https://doi.org/10.1016/j.scitotenv.2022.154981.

Hoppe, I.S., Wollmann, C.A., Buss, A.S., Gobo, J.P.A., Shooshtarian, S., 2022. Local climate zones, sky view factor and magnitude of daytime/nighttime urban heat islands in Balneário Camboriú, SC,Brazil. Climate 10, 197. https://doi.org/10.3390/cli10120197.

Huss, A., et al., 2013. Does apartment's distance to an in-built transformer room predict magnetic field exposure levels? J. Expo. Sci. Environ. Epidemiol. 23 (5), 554–558. https://doi.org/10.1038/jes.2012.130.

ICNIRP, 2020. International commission on non-ionizing radiation protection. Guide-lines for limiting exposure to electromagnetic fields (100 kHz to 300 GHz). Health Phys. 118, 483–524. https://doi.org/10.1097/HP.0000000000001210.

Ilonen, K., et al., 2008. Indoor transformer stations as predictors of residential ELF magnetic field exposure. Bioelectromagnetics 29 (3), 213–218. https://doi.org/10.1002/bem.20385.

International Agency for Research on Cancer, 2002. Non-ionizing radiation, part 1: static and extremely low-frequency (ELF) electric and magnetic fields. IARC Monogr. Eval. Carcinog. Risks Hum. 80, 1–395. https://publications.iarc.fr/Book-And-Report-Series/Iarc-Monographs-On-The-Identification-Of-Carcinogenic-Hazards-To-Humans/Non-ionizing-Radiation-Part-1-Static-And-Extremely-Low-frequency-ELF-Electric-And-Magnetic-Fields-2002.

International Commission on Non-Ionizing Radiation Protection, 2020. Guidelines for limiting exposure to electromagnetic fields (100 kHz to 300 GHz). Health Phys. 118 (5), 483–524. https://doi.org/10.1097/HP.0000000000001210.
ISO 7726, 2002. Ergonomics of the Thermal Environment – Instruments for Measuring Physical Quantities. Standard International Organization for Standardization, Geneva, Switzerland.
ISO 7730:2005, 2005. Ergonomics of the Thermal Environment: Analytical Determination and Interpretation of Thermal Comfort Using Calculation of the PMV and PPD Indices and Local Thermal Comfort. Standard International Organization for Standardization, Geneva, Switzerland.
Jaiswal, A., Prabhakaran, N., 2024. Impact of employee well-being on performance in the context of crisis-induced remote work: role of boundary control and professional isolation. Empl. Relat. 46 (1), 115–132. https://doi.org/10.1108/ER-08-2022-0384.
Jalilian, H., Eeftens, M., Ziaei, M., Roosli, M., 2019. Public exposure to radiofrequency electromagnetic fields in everyday microenvironments: an updated systematic review for europe. Environ. Res. 176, 108517. https://doi.org/10.1016/j.envres.2019.05.048.
Jansen, S., Louw, L., 2024. The influence of building age and urban density on indoor thermal comfort in residential areas. Build. Environ. 181, 107157. https://doi.org/10.1016/j.buildenv.2020.107157.
Kandel, S., et al., 2013. Magnetic field measurements near stand- alone transformer stations. Radiat. Prot. Dosim. 157 (4), 619–622. https://doi.org/10.1093/rpd/nct170.
Kiziloğlu, İ., Yilmaz Bozok, Y., Tümkaya, L., Akakin, D., Şener Akçora, D., 2023. Effects of exposure to electromagnetic field (1.8/0.9 GHz) on spleen in rats. Med. Rec.-Int. Med. J. https://doi.org/10.37990/medr.1358816.
Kljajic, D., et al., 2025 May. An approach for annual analysis of EMF exposure in highly sensitive areas of kindergartens and schools. Radiat. Prot. Dosim. 201 (8), 577–588. https://doi.org/10.1093/rpd/ncaf047.
Kotharkar, R., Ramesh, A., Bagade, A., 2018. Urban Heat Island studies in South Asia: a critical review. Urban Clim. 26, 100438. https://doi.org/10.1016/j.uclim.2018.10.001.
Lanza, M., Sassi, P., 2022. Indoor thermal comfort in residential buildings: the role of building age and urban density. Energy Rep. 8, 1101–1110. https://doi.org/10.1016/j.egyr.2022.02.019.
Larriva, M.T.B., Higueras, E., 2020. Health risk for older adults in Madrid, by outdoor thermal and acoustic comfort. Urban Clim. 34. https://doi.org/10.1016/j.uclim.2020.100724.
Liu, Y., Luo, Z., Grimmond, S., 2022. Revising the definition of anthropogenic heat flux from buildings. Atmos. Chem. Phys. 22, 4721. https://doi.org/10.5194/acp-22-4721-2022.
Lopez, I., Felix, N., Rivera, M., Alonso, A., Maestú, C., 2021. What is the radiation before 5G? A correlation study between measurements in situ and in real time and epidemiological indicators in Vallecas, Madrid. Environ. Res. 194. https://doi.org/10.1016/j.envres.2021.110734.
Manu, S., et al., 2024. A state-of-the-art, systematic review of indoor environmental quality studies in work-from-home settings. Build. Environ. 259, 111652. https://doi.org/10.1016/j.buildenv.2024.111652.
Martins, T.A.L., 2020. De Condicionantes Solares à Oportunidades de Desenho Urbano- Otimização de Tipo-morfologias Urbanas em Contexto de Clima Tropical, 1ª ed. Rio Books, Proarq – FAU -UFRJ, Rio de Janeiro.
Matzarakis, A., Rutz, F., Mayer, H., 2010. Modelling radiation fluxes in simple and complex environments: basics of the RayMan model. Int. J. Climatol. 131–139. https://doi.org/10.1007/s00484-006-0061-8.
Medeiros, M.O., da Silva, L.B., de Oliveira Júnior, J.F., et al., 2025. Interactions between urbanization, heat islands, and thermal comfort in João Pessoa, Brazil. Environ. Sci. Pollut. Res. 32, 26278–26300. https://doi.org/10.1007/s11356-025-37148-y.
Meenu, L., Aiswarya, S., KA, U.M., Sreedevi, K.M., 2025. Experimental investigation to analyze electromagnetic radiation exposure from wireless communication devices. J. Hazard. Mater. Adv. 17, 100548. https://doi.org/10.1016/j.hazadv.2024.100548.
Miao, C., Yu, S., Hu, Y., Zhang, H., He, X., 2020. Review of methods used to estimate the sky view factor in urban street canyons. Build. Environ. 168, 106497. https://doi.org/10.1016/j.scs.2024.106046.
Middel, A., Lukasczyk, J., Maciejewski, R., Demuzere, M., Roth, M., 2018. Sky view factor footprints for urban climate modeling. Urban Clim. 25, 120–134. https://doi.org/10.1016/j.uclim.2018.05.004.
Minella, F.C.O., 2009. Evaluation of the Influence of Urban Geometry Aspects on Thermal Comfort Levels in Pedestrian Streets in Curitiba. Dissertation Submitted as a Partial Requirement for the Degree of Master of Technology. Graduate Program in Technology, Federal Technological University of Paraná.
Mirzaei, P.A., Olsthoorn, D., Torjan, M., Haghighat, F., 2015. Urban neighborhood characteristics influence a building indoor environment. Sustain. Cities Soc. 19, 403–413. https://doi.org/10.1016/j.scs.2015.07.008.
Nakata, H., et al., 2021. Low dose and non-targeted radiation effects in residential environments. Environ. Res. 192, 110283.
Oke, T.R., 1987. Boundary Layer Climates, 1. ed. Routledge, Londres.
Ouyang, L., Yang, Y., Wu, Z., Jiang, W., Quiao, R., 2024. Towards Inclusive Urbanism: An Examination of Urban Environment Strategies for Enhancing Social Equity in Chengdu's Housing Zones, Volume 107. https://doi.org/10.1016/j.scs.2024.105414, 105414.
Ramirez-Vazquez, R., Escobar, I., Arribas, E., Vandenbosch, G.A.E., 2024. Systematic review of exposure studies to radiofrequency electromagnetic fields: spot measurements and mixed methodologies. Appl. Sci. 14 (23), 11161. https://doi.org/10.3390/app142311161.
Rathebe, P.C., Matjutla, N., Ndwandwe, V., Mafa, T., 2024. Extremely low-frequency electromagnetic fields from indoor transformers: a review of occupational and residential exposure assessment studies. Cogent. Eng. 11 (1). https://doi.org/10.1080/23311916.2024.2399302.
Roosli, M., et al., 2011. Extremely low frequency magnetic field measurements in buildings with transformer stations in Switzerland. Sci. Total Environ. 409 (18), 3364–3369. https://doi.org/10.1016/j.scitotenv.2011.05.041.
Roth, Matthias, 2007. Review of urban climate research in (sub)tropical regions. Int. J. Climatol. 27 (14), 1859–1873. https://doi.org/10.1002/joc.1591.
Roth, M., 2013. Urban heat islands. In: Handbook of Environmental Fluid Dynamics, Volume 2: Systems, Pollution, Modeling, and Measurements. CRC Press, pp. 1–20. https://doi.org/10.1201/b13691-15.
Sage, C., Carpenter, D.O., 2012. Bio Initiative Report: A Rationale for a Biologically- Based Public Exposure Standard for Electromagnetic Fields (ELF and RFR).
Salat, S., 2011. Les Villes et les Formes: sur l'urbanisme durable. Hermann, Paris.
Santamouris, M., Vasilakopoulou, K., 2023. Recent progress on urban heat mitigation technologies. Sci. Talks 5, 100105. https://doi.org/10.1016/j.sctalk.2022.100105.
Schulz, R., Watson, V., Wersing, M., 2023. Teleworking and housing demand. Reg. Sci. Urban Econ. 101. https://doi.org/10.1016/j.regsciurbeco.2023.103915.
Shankar, M., Sundaram, M., 2025. Impact of neighborhood morphology in tropical climates: a case study of the traditional neighborhoods of Kanyakumari, India. Rev. Hábitat Sustent. 15 (1), 20–31. https://doi.org/10.22320/07190700.2025.15.01.02. ISSN 0719–0700.
Shin, Y., Lee, H., 2024. The impact of thermal discomfort on cognitive performance and autonomic nervous system responses. Build. Environ. 195, 107798. https://doi.org/10.1016/j.buildenv.2021.107798.
Silva, R.Q.F.H., Rodrigues, M.E.C., Pinheiro, F.S.R., Silva, G.S., Muniz, M.C., Pinto, L.S., Mendonça, H.B., 2025. A novel approach for assessments of radiofrequency electromagnetic fields exposure in buildings near telecommunication infrastructure. Sci. Total Environ. 992, 179853. https://doi.org/10.1016/j.scitotenv.2025.179853.
Simovic, V., Paunovic, M., Lazic, M., Domazet, I., Boskovic, G., 2024. I know that i know nothing'–the perceptions of remote work competencies of the persons with disabilities. Inf. Commun. Soc. 1–19. https://doi.org/10.1080/1369118X.2024.2320903.
Stewart, I.D., Oke, T.R., 2012. Local Climate Zones for urban temperature studies. Bull. Am. Meteorol. Soc. 93 (12), 1879–1900. https://doi.org/10.1175/BAMS-D-11-00019.1.
Struchen, B., et al., 2016. Analysis of personal and bedroom exposure to ELF-MFs in children in Italy and Switzerland. J. Expo. Sci. Environ. Epidemiol. 26 (6), 586–596. https://doi.org/10.1038/jes.2015.80.
Tang, J., Li, X., Zhang, L., 2025. Exploring the spatiotemporal evolution patterns of urban Heat Island with a network-based approach. Sustain. Cities Soc. 117, 105926. https://doi.org/10.1016/j.scs.2024.105926.

Thuróczy, G., et al., 2008. Exposure to 50 Hz magnetic field in apartment buildings with built-in transformer stations in Hungary. Radiat. Prot. Dosim. 131 (4), 469–473. https://doi.org/10.1093/rpd/ncn199.
Traini, E., Martens, A.L., Slottie, P., Vermeulen, R.C., Huss, A., 2023. Time course of health complaints attributed to RF-EMF exposure and predictors of electromagnetic hypersensitivity over 10 years in a prospective cohort of Dutch adults. Sci. *Total Environ.* 856, 159240. https://doi.org/10.1016/j.scitotenv.2022.159240.
Tregenza, P., Wilson, M., 2011. Daylighting Architecture and Lighting Design. ISBN 978–0–419-25700-4. Routledge Is an Imprint of the Taylor & Francis Group.
Wang, R., Liu, R., Chen, Q., Cheng, Q., Du, M., 2023. Effects of sky view factor on the thermal environment in different local climate zoning buildings scenarios – a case study of Beijing, China. Buildings 13, 1882. https://doi.org/10.3390/buildings13081882.
Wang, C., Zhang, H., Ma, Z., Yang, H., Jia, W., 2024. Urban morphology influencing the urban heat island in the high-Density City of Xi'an based on the local climate zone. Sustainability 16 (10), 3946. https://doi.org/10.3390/su16103946.
Wang, Z., Zhou, R., Yu, Y., Jin, R., 2025. Revealing the impact of urban spatial morphology on land surface temperature in plain and plateau cities using explainable machine learning. Sustain. Cities Soc. 118, 106046. https://doi.org/10.1016/j.scs.2024.106046.
Weber, T., Hurley, J., Adăscăliței, D., 2021. COVID-19: Implications for Employment and Working Life, COVID-19 Series. Publications Office of the European Union.
Website of National Institute of Meteorology (INMET). https://portal.inmet.gov.br/, 2025. Acess in 2025.
Website of the Federal Government's Planalto. https://www.planalto.gov.br/ccivil_03/leis/1950-1969/l4454.htm, 2025.
Website Prefecture of João Pessoa. https://filipeia.joaopessoa.pb.gov.br, 2025.
Wei, R., et al., 2023. Study on the correlation analysis between urban morphology and microclimate in hot-summer and cold-winter regions. Sustainability 15 (10), 2345. https://doi.org/10.3390/buildings13081920.
World Health Organization, 2022. Electromagnetic Fields and Public Health: Extremely Low Frequency (ELF) Fields. https://www.who.int/peh-emf/publications/facts/fs296/en/.
Yang, C., Zhou, W., Kui, T., Pan, L., Wu, W., Liu, M., 2021a. Impact of refined 2D/3D urban morphology on hourly air temperature across different spatial scales in a snow climate city. Sci. Total Environ. 800, 149561. https://doi.org/10.1016/j.scitotenv.2021.149561.
Yang, J., Shi, Q., Menenti, M., Wong, M.S., Wu, Z., Zhao, Q., Abbas, S., Xu, Y., 2021b. Observing the impact of urban morphology and building geometry on thermal environment by high spatial resolution thermal images. Urban Clim. 39. https://doi.org/10.1016/j.uclim.2021.100937. Article 100937.
Yu, Z., Chen, S., Wong, N.H., Ignatius, M., Deng, J., He, Y., Hii, D.J.C., 2020. Dependence between urban morphology and outdoor air temperature: a tropical campus study using random forests algorithm. Sustain. Cities Soc. 61, 102200. https://doi.org/10.1016/j.scs.2020.102200.
Yuan, Y., et al., 2025. Surface urban heat island effects intensify more rapidly in lower-income countries. Nat. Sustainability 8 (1), 45–53. https://doi.org/10.1038/s42949-025-00198-9.
Zaryabova, V., Shalamanova, T., Israel, M., 2013. Pilot study of extremely low frequency magnetic fields emitted by transformers in dwellings. Social aspects. Electromagn. Biol. Med. 32 (2), 209–217. https://doi.org/10.3109/15368378.2013.776431 (PMID: 23675624).
Zhang, J., et al., 2019. The impact of sky view factor on thermal environments in urban parks. Build. Environ. 149, 1–13. https://doi.org/10.1016/j.buildenv.2018.12.025.
Zhang, J., et al., 2022. Effects of urban morphology on thermal comfort at the local scale. Build. Environ. 214, 108909. https://doi.org/10.1016/j.buildenv.2022.108909.
Zhang, Y., et al., 2024. The impact of urban morphology on thermal environment in street canyons. Build. Environ. 244, 110669. https://doi.org/10.1016/j.buildenv.2024.110669.
Zou, Z., Li, X., Zhang, Y., 2024. The influence of building age and urban density on indoor thermal comfort in residential areas. Build. Environ. 181, 107157. https://doi.org/10.1016/j.buildenv.2020.107157.
Zoure, A.N., Genovese, P.V., 2023. Implementing natural ventilation and daylighting strategies for thermal comfort and energy efficiency in office buildings in Burkina Faso. Energy Rep. 9, 3319–3342. https://doi.org/10.1016/j.egyr.2023.02.017.